ELSEVIER

PII: S0032-3861(97)10185-9

Polymer Vol. 30 No. 25, pp. 6301–6307, 1998

0032-3861/98/$ - see front matter

Gelation mechanism of thermoreversible poly(vinylidene fluoride) gels in glyceryl tributyrate†

Sukumar Mal and Arun K. Nandi*

Polymer Science Unit, Indian Association for the Cultivation of Science, Jadavpur, Calcutta 700 032, India

(Received 23 January 1997; revised 20 August 1997; accepted 10 September 1997)

Poly(vinylidene fluoride) (PVF_2) gels in glyceryl tributyrate (GTB) with fibrillar morphology in the dried state. The gels are transparent and WAXS results indicate the presence of α-phase PVF_2 crystals in the gels. The gelation rate (t_{gel}^{-1}) has been measured by the test tube tilting method and has been analysed with the equation $t_{gel}^{-1} \propto f(c)f(T)$, where $f(c)$ = concentration function and $f(T)$ = temperature function. At a fixed temperature, the variation of t_{gel}^{-1} with concentration suggests that the nature of the connectedness in this system obeys the three dimensional percolation mechanism. On the other hand, at a fixed concentration, the variation of the gelation rate with temperature suggests that the gelation is a two step concerted process of conformational ordering and crystallization, the former acting as the rate determining step. The formation of fibrillar gels in this system has been attributed to the solvation of the TGTG conformer of PVF_2 through compound formation in a 3:1 molar ratio of the monomeric units of PVF_2 and GTB.

(Keywords: thermoreversible gels; poly(vinylidene fluoride); glyceryl tributyrate)

INTRODUCTION

Recently, studies on the thermoreversible gelation of poly(vinylidene fluoride) (PVF_2) have gained considerable momentumbibr[1–3] because of the piezo and pyroelectric properties of the polymer[4]. Different polymorphs of PVF_2 are produced during the gelation and different mechanisms have been proposed for the gelation processes[1–3]. Crystallization is the cause of gelation for PVF_2 gels in acetophenone and in ethyl benzoate[2], whereas liquid–liquid phase separation has been considered as the cause of gelation for PVF_2 gels in γ-butyrolactone[1,3]. The morphology of these gels after drying is spheroidal as evidenced from scanning electron micrographs[1,3,5]. Here, we report a PVF_2 gel whose morphology in the dried state is not spheroidal but fibrillar in nature. We believe that the morphologies of the gels will not be affected much due to drying and, therefore, we assume throughout the rest of the paper that the undried gels possess the same types of morphology as the dried gels.

Elucidation of the gelation mechanism of thermoreversible polymeric gels is a main problem in condensed polymer systems and various sophisticated techniques are used for this purpose[6–11]. The mechanism of thermoreversible gelation is usually described in two ways: (a) a macroscopic mechanism and (b) a microscopic mechanism. The former deals with the nature of the connectedness (physical crosslinking) whereas the latter sheds light on the mechanism by which the physical crosslinking occurs. The gelation rate may be used to delineate both mechanisms, along with other techniques[2]. It is usually expressed as a combination of concentration function $f(c)$ and temperature function $f(T)$[2,13]:

$$t_{gel}^{-1} \propto f(c)f(T) \quad (1)$$

where t_{gel} is the gelation time and t_{gel}^{-1} is usually expressed as the gelation rate. By keeping $f(T)$ constant, the dependence of the gelation rate on the concentration yields the macroscopic mechanism of gelation. On the other hand, by keeping $f(c)$ constant and studying the variation of the gelation rate with temperature, the microscopic mechanism of gelation can be explored[2,3,13], with the help of other techniques. In our previous work[2] we have shown from the variation of t_{gel}^{-1} with $f(c)$ (equation (1)) that the PVF_2 gels in acetophenone and in ethyl benzoate obey a three dimensional percolation model. Also, from the temperature dependence of the gelation rate it has been concluded that crystallites are involved in the formation of the three dimensional crosslinking.

The purpose of the present study is to elucidate both the macroscopic and microscopic mechanisms of PVF_2 gels in glyceryl tributyrate (GTB). Since the morphology of these gels is quite different from the PVF_2 gels so far studied[1–3], it is important to know the mechanism by which the fibrillar gels of PVF_2 are produced and also whether the percolation mechanism of gelation is suitable for the formation of these fibrillar gels. Apart from the gelation rate measurement, wide angle X-ray scattering (WAXS), scanning electron microscopy (SEM), and differential scanning calorimetry (d.s.c.) have been used to elucidate the mechanism of gelation.

EXPERIMENTAL

Three commercial PVF_2 samples—Sol-10, Sol-12 and KY-201—are used in this work. The characteristics of the samples are presented in *Table 1*[2]. The samples are

* To whom correspondence should be addressed
† Partly presented at Europhysics conference on polymer–solvent complexes and intercalates, Meyrueis (France), July 1–5, 1996

Table 1 Characteristics of the samples

Sample	$\bar{M}_w$ [a] $\times 10^5$	PDI [b]	H–H defect [c] (mol. %)
Sol-10	4.48	2.09	4.19
Sol-12	7.74	2.57	4.06
KY-201	8.81	2.89	5.31

[a] Weight average molecular weight
[b] PDI = polydispersity index
[c] H–H defect = Head to Head defect

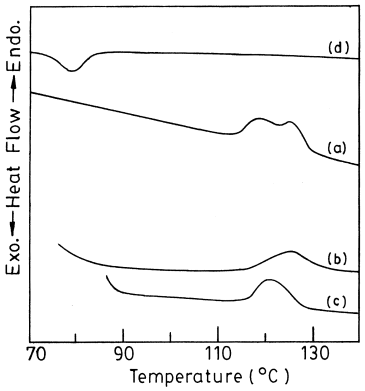

Figure 1 Representative d.s.c. thermograms of PVF_2 (KY-201)–GTB gels (4 g/dL) prepared at (a) 50°C (H.R. = 10°/min), (b) 50°C (H.R. = 40°/min), (c) 80°C (H.R. = 10°/min), (d) dynamic cooling (5°/min) from 180°C

recrystallized from dilute solution (~0.3% w/v) in acetophenone, washed repeatedly with methanol and finally dried in vacuum at 60°C for three days. The Sol-10 and Sol-12 PVF_2 samples are chosen to investigate the influence of molecular weight on the gelation mechanism, whereas the KY-201 and Sol-12 samples are chosen to study the influence of chain structure [Head to Head (H–H) defect] on the gelation mechanism of PVF_2. The solvent, glyceryl tributyrate (GTB) (Sigma, USA), is used as received.

The gels are usually prepared in sealed glass tubes except for the gels used in thermal measurement. Appropriate amounts of polymer and solvent are taken in glass tubes, degassed by a freeze–thaw technique and are sealed in vacuum (10^{-3} mm Hg). The solutions are homogenized at 180°C and are quenched to the desired temperature for gelation. The gelation rates are measured by the test-tube tilting method[1–3,13–16]†. For the SEM study the gels are removed from the sealed tubes, dried at 50°C under vacuum, gold coated and then micrographs are taken through a SEM apparatus (Hitachi, S-415A). For the WAXS study a Philips powder diffraction apparatus (model PW1710) is used with nickel filtered Cu K_α radiation. The same mass of the freshly prepared gel for each sample is taken into the same glass groove and the instrument is scanned from 10° to 45° at the rate of 0.9°, 2θ per min.

The thermal study of the gels has been done using a Perkin–Elmer differential scanning calorimeter (DSC-7) fitted with a 3700 data station. The instrument is calibrated with indium before use. Measured quantities of polymer and solvent are put into LVC capsules fitted with o-rings to prevent any solvent loss during heating. The samples are melted at 180° and homogenized by shaking. Then they are quenched to the desired gelation temperature. After standing for a definite time (3 hrs) for each sample the instrument is scanned at the rate of 10°/min. The peak temperature(s) have been taken as the gel melting temperature(s). In some cases, the d.s.c. thermograms exhibit two melting peaks due to melt recrystallization. So, for the comparison of enthalpy of fusion (ΔH) values, they are measured by heating at a higher heating rate (40°/min) from the gelation temperature (90°C) to 180°C. The enthalpy of gel formation is measured from the exotherm obtained by cooling a homogeneous solution from 180°C at the rate of 5°C/min. In *Figure 1* representative d.s.c. thermograms for gel fusion and gel formation are presented.

† Perfection in the rate measurement has been arrived at up to $t_{gel} = \pm 5$ sec by a trial and error procedure.

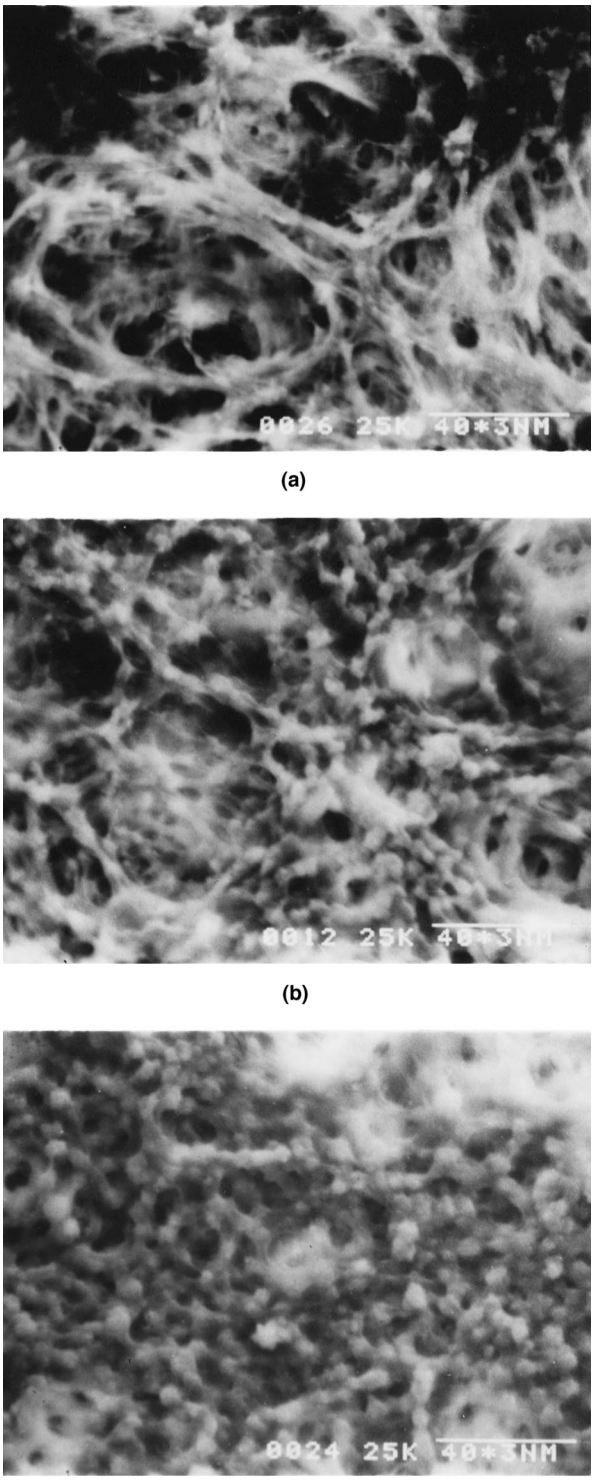

Figure 2 Scanning electron micrographs of PVF_2 (KY-201) gels (4 g/dL) in: (a) GTB, (b) ethyl benzoate and (c) acetophenone

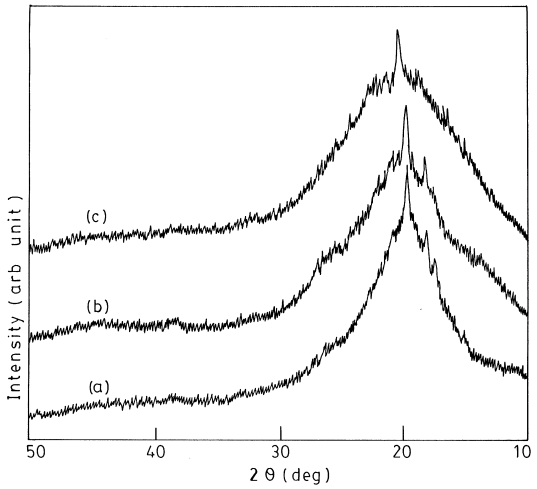

Figure 3 WAXS diffractograms of nascent PVF_2 (KY-201) gels (6 g/dL) in: (a) GTB, (b) ethyl benzoate and (c) acetophenone

Table 2 d_{hkl} (Å) of α-phase KY-201 PVF_2 gels in GTB

Solvent	d_{110}	d_{200}	d_{010}
GTB	4.50	4.88	5.06
Acetophenone	4.46	4.82	—
Ethyl benzoate	4.46	4.84	5.00
Melt	4.43	4.82	5.00

RESULTS AND DISCUSSION

Morphology and structure

The PVF_2 gels in GTB are transparent at all the gelation temperatures studied here. This is in sharp contrast to the PVF_2 gels in acetophenone or in ethyl benzoate where they are turbid in nature[2]. In *Figure 2* the SEMs of dried PVF_2 gels in GTB, acetophenone and ethyl benzoate are compared for the KY PVF_2 at the same magnification. It is apparent from the Figure that in the former solvent the gels have fibrillar morphology. In the latter two cases the gels have spheroidal morphology, though in the ethyl benzoate system some fibrillar morphology is also found. In *Figure 3* the WAXS patterns of the freshly prepared gels of the three systems are compared. It is clear from the Figure that the overall nature of the X-ray pattern is the same for the three solvents, indicating the presence of α-phase crystals[17,18] of PVF_2 in the gels. However, there is a gradation in the broadening of the amorphous scattering (lower) zone and it follows the order acetophenone > ethyl benzoate > GTB. The polymer solvent interaction parameter (χ) of the three solvents is determined using the depression of the equilibrium dissolution temperature[2,19] and has been found to be 0.09, 0.31 and 0.39, for acetophenone, ethyl benzoate and GTB, respectively. So the broadening order of the amorphous scattering is in accordance with the χ parameter values. From the peak position, d_{hkl} values are calculated and are presented in *Table 2*. The d_{hkl} values of the acetophenone and ethyl benzoate systems are the same as those of pure PVF_2 crystallized from the melt. On the other hand, the d_{hkl} values of GTB are slightly higher than the others, indicating a small expansion of the unit cell. This small expansion of the unit cell may be due to the fibrillar nature of the crystal[20], where a larger fraction of H–H defects enter into the lattice causing the unit cell expansion[21,22].

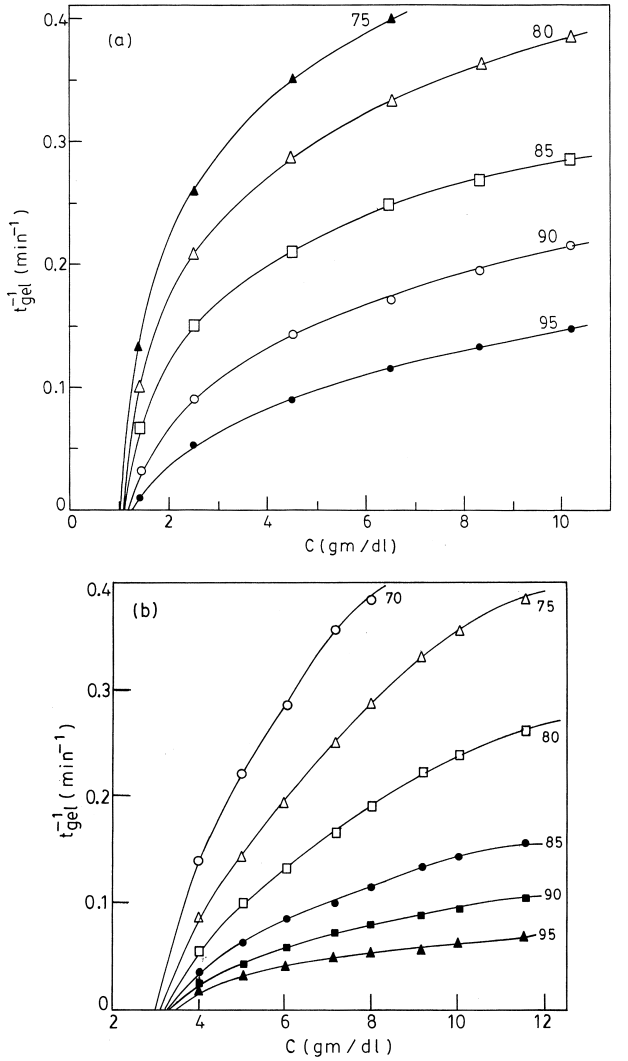

Figure 4 (a) t_{gel}^{-1} *versus* concentration plot of KY-201 PVF_2 in GTB at indicated temperatures (°C). (b) t_{gel}^{-1} *versus* concentration plot of Sol-12 PVF_2 in GTB at indicated temperatures (°C)

Gelation rate

Figures 4a and *b* represent the gelation rate–concentration diagrams of PVF_2-GTB systems at indicated gelation temperatures (T_{gel}). At a particular T_{gel} the gelation rate increases in a nonlinear way with concentration but at higher concentrations it slowly levels up. At a fixed concentration the gelation rate gradually decreases with increase in temperature. To explain the concentration and temperature dependency of the gelation rate, an explicit expression (equation (1)) is necessary. Earlier[2], it has been shown that $f(c) \propto \phi^n$ where ϕ is the reduced overlapping concentration and is equal to $[C - C^*_{t=\alpha}(T)]/C^*_{t=\alpha}(T)$; $C^*_{t=\alpha}(T)$ is the critical gelation concentration at temperature T and can be measured from the extrapolation of the plots of *Figures 4a* and *b* to the zero gelation rate; 'n' is an exponent and it has been argued that it is equal to the percolation exponent β of the expression[23,24]:

$$G = (P - P_c)^{\beta} \qquad (2)$$

where G is the gel fraction, P is the conversion factor and P_c is its critical value. The nature of $f(T)$ is dependent on the process by which gelation occurs. Since gelation may occur through crystallization[2,13], coil to helix transition[10,25,26], spinodal decomposition[27,28] etc., $f(T)$ cannot be given a

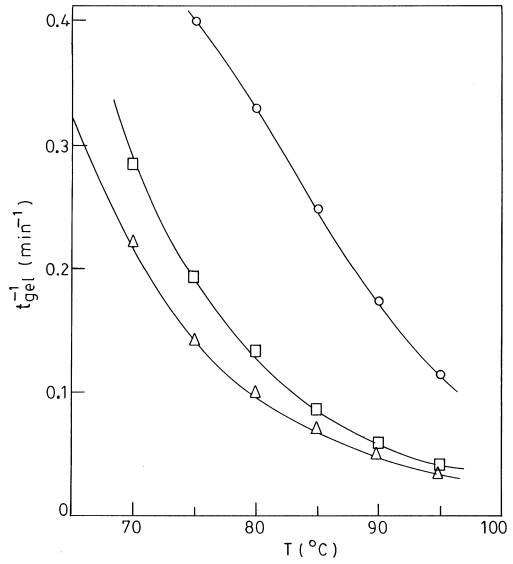

Figure 5 t_{gel}^{-1} *versus* temperature plot of PVF_2 (6 g/dL) in GTB : ○—Ky-201, □—Sol-12 and △—Sol-10

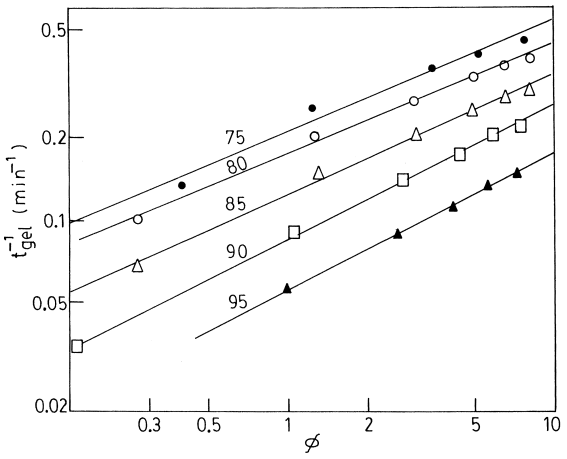

Figure 6 $\log t_{gel}^{-1}$ *versus* $\log \phi$ plot of KY-201 PVF_2 gels in GTB at indicated temperatures (°C)

generalized form. Details of these functions will be discussed later.

In *Figure 5* the gelation rates of different PVF_2 samples are compared for a 6% (w/v) solution at different gelation temperatures. It is clear from the Figure that the higher molecular weight PVF_2 sample has the higher gelation rate. This is because the critical gelation concentration for the higher molecular weight sample is lower than that of the lower molecular weight sample[2,29]. Consequently, ϕ has a higher value for the same concentration yielding a higher gelation rate. Like the PVF_2 gels in acetophenone or in ethyl benzoate, here also the higher H–H defect content KY-201 PVF_2 has a higher gelation rate than the others. The reason for this higher rate will be presented later.

The concentration function (f(c))*: percolation mechanism*

At a fixed temperature equation (1) can be expressed as

$$t_{gel}^{-1} \propto \phi^n \tag{3}$$

and, therefore, *n* can be measured from the slope of double logarithmic plots of t_{gel}^{-1} and ϕ. In *Figure 6* representative plots are shown for the KY-201 PVF_2 sample at indicated T_cs. It is clear from the Figure that the data are very well

Table 3 Exponent '*n*' values of PVF_2 gels in GTBdetermined from least square slopes of doublelogarithmic plots of t_{gel}^{-1} and ϕ

Temp. (°C)	KY-201	Sol-10	Sol-12
70	—	0.64	0.62
75	0.40	0.64	0.64
80	0.40	0.65	0.63
85	0.43	0.63	0.61
90	0.49	0.56	0.56
95	0.50	0.51	0.50
Av.	0.44	0.60	0.59
St. Dev.	0.05	0.05	0.05

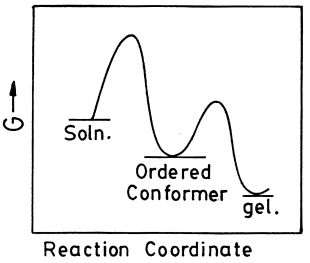

Figure 7 Schematic representation of Gibbs free energy (*G*) *versus* reaction coordinate of the gelation process

fitted by a straight line for each temperature. The slopes of these plots for all the PVF_2 samples are presented in *Table 3* and vary from 0.40 to 0.64. The values are very similar to those obtained for PVF_2-acetophenone and PVF_2-ethyl benzoate gels and are close to the β value (0.45) for percolation in the three dimensional lattice. Thus, the exponent value is independent of the morphology of the gel and is completely different from the value '2' as proposed by Ohkura *et al.*[13]. It is also much lower than the classical value of unity, where gelation has been considered as a chain reaction[30,31]. Recently, Pekcan *et al.*[32] observed an '*n*' value equal to 0.38 during sol–gel transitions by free radical crosslinking copolymerization using a fluorescence technique. Therefore, it can be concluded that gelation, in general, obeys the three dimensional percolation mechanism and '*n*' in equation (3) may be replaced by 0.45.

The temperature function

When a polymer solution is cooled conformational changes occur[11]. Since the WAXS of the gels corresponds to the α-phase of PVF_2, it is evident that the PVF_2 coil first adopts the TGTG conformation and this conformer then produces the fibrillar α-crystallites, causing gelation. Schematically

$$\text{Coil} \rightarrow \text{TGT}\bar{\text{G}} \text{ conformer} \rightarrow \underset{\text{(fibrillar gel)}}{\alpha \text{ crystallites.}} \tag{4}$$

Since the formation of fibrillar α-PVF_2 is very uncommon we want to search for the cause of inhibition of the chain folding process to produce the fibrillar gels. In most gelation processes solvent molecules form compounds with the conformer and thereby prevent chain folding yielding fibrillar morphology of the gels[9,12,26,33,34]. As an evidence of the compound formation the enthalpy of gel fusion and the enthalpy of gel formation show a maximum with composition. In this system we also observed from the enthalpy *versus* composition plot an evidence of compound formation at a weight fraction of $PVF_2 = 0.40$. This corresponds to the molar ratio of 3:1 for the PVF_2 segment and GTB respectively[35]. The dipole–dipole interaction[36,37] of three >C=O groups of GTB and $>CF_2$ group of each monomeric unit of PVF_2 is

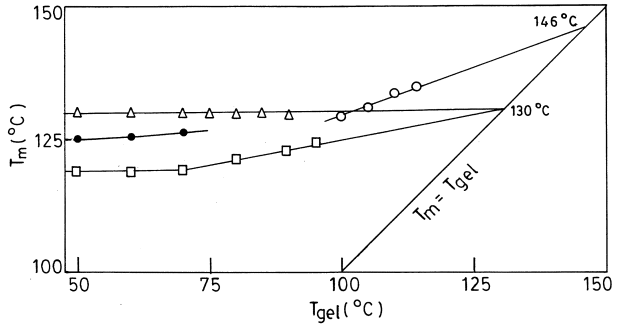

Figure 8 Hoffman–Weeks plots of gel melting temperature and crystal dissolution temperature of KY-201 PVF_2 gels (4 g/dL). □—T_{gm} by d.s.c., ●—T_{gm} 2nd peak (d.s.c.), △—T_{gm} by test tube tilting method, and ○—dissolution temperature by d.s.c.

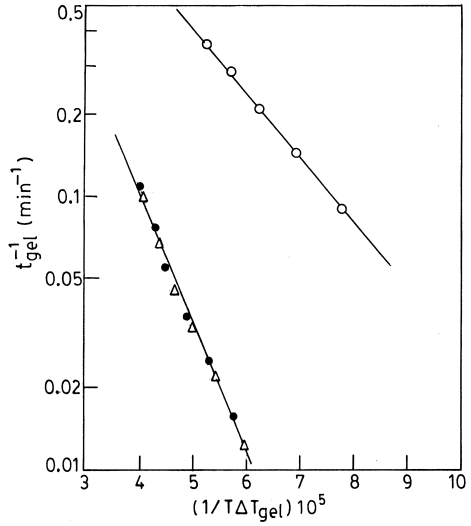

Figure 9 Log t_{gel}^{-1} *versus* $1/T\Delta T_{gel}$ plots of PVF_2 gels (4 g/dL) in GTB: ○—KY-201, ●—Sol-12 and △—Sol-10

responsible for the compound formation which causes the inhibition of chain folding. As shown in equation (4) the gelation is a two step process[25] and each step has its own activation energy (*Figure 7*). So, it is necessary to make a temperature coefficient analysis for both the processes.

Conformational ordering. Flory and Weaver[38] gave an expression for the rate constant (K) for conformational ordering from coil to helix of a dilute aqueous collagen solution:

$$K = \text{const. } \exp(-A/kT\Delta T) \qquad (5)$$

where $A = 2\sigma\Delta F/\Delta S$, σ is the surface energy in the new surface produced due to conformational ordering, ΔF is the free energy of activation at the melting temperature per repeating unit and ΔS is the overall entropy change per repeating unit for the conformational transition. Though originally it was believed that PVF_2 in the α-phase crystallizes in a 2_1 helical structure with an alternating *cis* and *trans* conformation, extensive research in this field suggests that TGTG is the appropriate conformation in the α-phase[39]. However, the above expression for the rate constant of the coil to helix transition can be applied to any change in conformation forming an ordered conformer. This is because, like a helix, this TGTG conformer also produces a new surface, different from the melt, with surface energy σ, and there will be a loss of entropy for the formation of the ordered conformer. The absolute values of σ, ΔS and ΔF may vary from conformer to conformer producing an ordered structure. Since, in the gelation process, conformational ordering is the first step, the gelation rate can be expressed as:

$$t_{gel}^{-1} = \text{const. } \exp(-A/kT\Delta T_{gel}) \qquad (6)$$

for a particular concentration. To analyse the gelation rate the equilibrium gel melting temperature (T_{gm}^0) is needed to calculate ΔT_{gel} ($=T_{gm}^0 - T$), and to measure T_{gm}^0 the Hoffman–Weeks procedure[40] for measuring the equilibrium melting point (T_m^0) of polymer crystals has been applied and is shown in *Figure 8*. In the Figure, the gel melting temperature (T_{gm}) obtained by d.s.c. and also by the test tube tilting method are presented. It is apparent from *Figure 8* that at some gelation temperatures (T_{gel}) two melting peaks are observed due to melt recrystallization, but at higher T_{gel} it shows one peak. Extrapolation of this plot to the $T_m = T_{gel}$ line corresponds to an equilibrium melting point T_{gm}^0 equal to 130°C. The gel melting temperature determined by the test tube tilting method when extrapolated also gives T_{gm}^0 at 130°C‡. But at higher temperatures no gel is produced; rather solution crystals are produced[16]. The melting points of the solution crystals are dependent on T_c and extrapolation of this plot yields the equilibrium dissolution temperature (T_d^0). T_d^0 is approximately equal to the value obtained by the visual method[2,19]. So there are two equilibrium melting points: (1) T_{gm}^0 and (2) T_d^0. Now the question is why two equilibrium melting points arise in the same system. The reason is the critical gelation concentration which increases with increase in temperature (*Figure 4*)[2,15]. At higher temperatures, therefore, though crystals are produced no gelation occurs even after ageing the solution for 7 days. Taking these T_{gm}^0s, log t_{gel}^{-1} has been plotted against $1/T\Delta T_{gel}$ and is shown in *Figure 9*. The data fit a straight line very well. From the least square slopes of these lines the '*A*' values are calculated and are presented in *Table 4*. It is clear from the Table that KY-201 PVF_2 gels have a lower A value than the others, explaining their higher gelation rate compared to the other samples at a particular temperature. The ΔF values are calculated taking the experimental lateral surface free energy (σ) values of each sample from a crystallization kinetic study[41,42] and taking ΔS equal to $\Delta H_u^0/C_\alpha$[43], where ΔH_u^0 = enthalpy of fusion (1.6 kcal/mol) and C_α is the chain characteristic ratio (5.5)§ of PVF_2. The ΔF values calculated from these results are also presented in *Table 4* and they vary from 11 to 14 kcal/mol, quite a reasonable value to permit the individual isolation of the conformers[45]. Moreover, from the potential energy diagrams of the isolated PVF_2 chain the energy barrier between the lowest and the highest energy conformers is about 9 kcal/mol[46]. The ΔF value shows a composition dependency; the higher the polymer concentration, the higher is its value. However, extrapolation of these values to zero polymer concentration yields $\Delta F = 9$–10 kcal/mol. So the ΔF values are in good agreement with the theoretical potential energy barrier of the isolated PVF_2 chain. This analysis of the gelation rate supports the view that conformational ordering is the first step for this gelation process.

‡ The gel melting temperature determined by this method corresponds approximately to the peak end temperature of the 2nd peak in d.s.c. thermograms.

§ The C_α value of the PVF_2 chain ($C_\alpha = \bar{r}_0^2/nl^2$, where $\bar{r}_0^2$ is the mean square unperturbed end-to-end distance, n is the number of segments, and l is the length of each monomeric unit) has been calculated taking the mean square unperturbed dimension ($\bar{r}_0^2/\bar{M} = 4.1 \times 10^{-17}$ cm^2) from viscosity results[44].

Table 4 '*A*' and ΔF values of PVF_2 gels in GTB

KY-201				Sol-10				Sol-12			
Conc. g/dL	T_{gm}^0 °C	*A* kcal/mol	ΔF kcal/mol	Conc. g/dL	T_{gm}^0 °C	*A* kcal/mol	ΔF kcal/mol	Conc. g/dL	T_{gm}^0 °C	*A* kcal/mol	ΔF kcal/mol
4.3	130	106.3	11.2	4.2	141	226.3	10.8	4.0	142	233.2	11.1
6.6	132	110.5	11.6	7.0	144	247.5	11.8	7.1	144	283.4	13.5
10.1	135	113.6	11.9	10.1	146	280.1	13.4	10.1	146	306.8	14.6

Table 5 $\sigma_u^2\sigma_e$ values (in erg^3/cm^6) of different PVF_2 samples in GTB gels

KY-201				Sol-10				Sol-12			
Conc. g/dL	T_d^0 °C	$\sigma_u^2\sigma_e$	$\sigma_\pm$ erg/cm^2	Conc. g/dL	T_d^0 °C	$\sigma_u^2\sigma_e$	$\sigma_\pm$ erg/cm^2	Conc. g/dL	T_d^0 °C	$\sigma_u^2\sigma_e$	$\sigma_\pm$ erg/cm^2
4.3	144	319.6	6.8	4.2	151	592.6	8.4	4.0	152	581.9	8.3
6.6	145	324.7	6.9	7.0	152	573.8	8.3	7.1	153	652.8	8.7
10.1	145	301.2	6.7	10.1	152	636.7	8.6	10.1	153	644.6	8.6
100.0 (from melt)	178	305.0	6.7	—	—	—	—	100.0	205	863.0	9.5

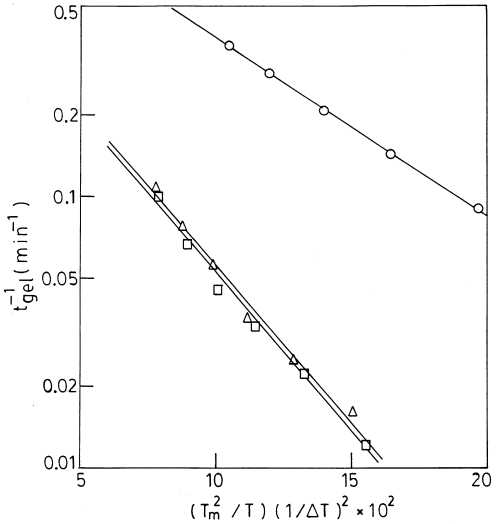

Figure 10 Log t_{gel}^{-1} *versus* $(T_m^2/T)(1/\Delta T)^2$ plots of PVF_2 gels (4 g/dL) in GTB: ○—KY-201, △—Sol-12 and □—Sol-10

Aggregation of ordered conformers producing fibrillar crystals. Due to the cohesive force of attraction and adequate symmetry of the ordered conformers they immediately undergo crystallization. Since crystallization is a nucleation controlled process, gelation is also a nucleation controlled process[2]. Therefore,

$$t_{gel}^{-1} = \text{Const. } v_2 \exp\left[\frac{E_D(v_2) - \Delta F^*(v_2)}{kT}\right] \qquad (7)$$

where v_2 is the volume fraction of polymer, $E_D(v_2)$ and $\Delta F^*(v_2)$ denote the free energy of transport and free energy for the formation of a critical size of nucleus, respectively, and

$$\Delta F^*(v_2) = \frac{8\pi\sigma_u^2\sigma_e - 4\pi kT\sigma_u^2 \ln v_2}{(\Delta H_u^0 \Delta T)^2} (T_d^0)^2 \qquad (8)$$

where σ_u and σ_e are the lateral and end surface free energies, and $\Delta T = T_d^0 - T$. In *Figure 10* t_{gel}^{-1} has been plotted against $(T_d^0)^2/T\Delta T^2$ and straight lines are observed. This supports the idea that the gelation is a nucleation controlled process. At a first approximation, the slope values of the plots are equated to $8\pi\sigma_u^2\sigma_e/\Delta H_u^2$ as earlier[2], and $\sigma_u^2\sigma_e$ values are calculated. In *Table 5* $\sigma_u^2\sigma_e$ and the mean interfacial energy values ($\sigma_\pm$) are presented. The values are very close to those of the PVF_2/acetophenone and PVF_2/ethyl benzoate gels and are also close to those of the pure PVF_2 samples[2]. These results, therefore, conclude that crystallization is the 2nd or final step in the gelation process.

Now to conclude this section one must know the activation energy value of the crystallization process. At the lowest undercooling studied here, for a 4% solution, $\Delta f^*(v_2)$ calculated from equation (8) has values of 6.8 and 7.0 KCal/mol for KY-201 and sol.-PVF_2 samples, respectively. At higher undercooling and also for higher concentration, this activation energy decreases for each system. Consequently, in comparison with the activation energy of the conformational ordering, the activation energy of crystallization is less. Therefore, crystallization follows immediately and it is difficult to distinguish the process responsible for gelation. So, gelation occurs here by a concerted two step process, the conformational ordering being the rate determining step.

CONCLUSIONS

From the study it can be concluded that PVF_2 gels in GTB with fibrillar morphology. The formation of this fibrillar morphology is believed to be due to the dipole–dipole interaction of the >C=O group of the ester and the $>CF_2$ group of the PVF_2 chain, making a compound at a 3:1 molar ratio of each PVF_2 segment and GTB. Analysis of the gelation rate yields that the nature of the connectedness in this system obeys the three dimensional percolation mechanism and gelation in this system is a concerted two step process of conformational ordering and crystallization, the former acting as the rate determining step.

ACKNOWLEDGEMENTS

We acknowledge Dr. P. Maiti and Mr. A. Dikshit for helping in d.s.c. and X-ray measurements. We also acknowledge the University Grants Commission, New Delhi for awarding the F.I.P. fellowship to one of us (S. M.).

REFERENCES

1. Cho, J. W., Song, H. Y. and Kim, S. Y., *Polymer*, 1993, **34**, 1024.
2. Mal, S., Maiti, P. and Nandi, A. K., *Macromolecules*, 1995, **28**, 2371.

3. Cho, J. W. and Lee, G. W., *J. Polym. Sci.*, 1996, **B34**, 1605.
4. Wang, T. T., Herbert, J. M. and Glass, A. M., *The Application of Ferroelectric Polymers*. Blackie and Sons Ltd., London, 1988.
5. Mal, S., Ph.D Thesis, Jadavpur University, 1997.
6. Grirolomo, M., Keller, A., Miyasake, K. and Overbag, N. J., *J. Polym. Sci.*, 1976, **B14**, 39.
7. Russo, P. S. (ed.), *Reversible Polymeric Gels and Related Systems*. Am. Chem. Soc., Washington DC, 1987.
8. Guenet, J. M., *Macromolecules*, 1986, **19**, 1961.
9. Guenet, J. M. and McKenna, G. B., *Macromolecules*, 1988, **21**, 1752.
10. Itagaki, H. and Takahashi, I., *Macromolecules*, 1995, **28**, 5477.
11. Kobayashi, M., Yoshioka, T., Masayuki, I. and Itoh, Y., *Macromolecules*, 1995, **28**, 7376.
12. Daniel, Ch., Deluca, M. D., Guenet, J. M., Brulet, A. and Menelle, A., *Polymer*, 1996, **37**, 1273.
13. Ohkura, M., Kanaya, T. and Kaji, K., *Polymer*, 1992, **33**, 5044.
14. Tan, H. M., Hiltner, A., Moet, A. and Baer, E., *Macromolecules*, 1983, **16**, 28.
15. Domszy, R. C., Alamo, R., Edwards, C. O. and Mandelkern, L., *Macromolecules*, 1986, **19**, 310.
16. Prasad, A. and Mandelkern, L., *Macromolecules*, 1990, **23**, 5041.
17. Lando, J. B. and Doll, W. W., *J. Macromol. Sci. Phys.*, 1968, **B2**, 205.
18. Hasegawa, R., Takahashi, Y., Chatani, Y. and Tadokoro, H., *Polymer J.*, 1972, **3**, 600.
19. Mal, S. and Nandi, A. K., in preparation.
20. Keller, A., in *Structure–Property Relationships of Polymeric Solvents*, ed. A. Hiltner. Plenum Press, New York, 1983, p. 25.
21. Datta, J. and Nandi, A. K., *Polymer*, 1994, **35**, 4812.
22. Datta, J. and Nandi, A. K., *Polymer*, 1997, **38**, 2719.
23. Stauffer, D., Coniglio, A. and Adam, M., in *Advances in Polymer Science*, Vol. 44, ed. K. Dusck. Springer–Verlag, Berlin, 1982, p. 103.
24. Zallen, R., *The Physics of Amorphous Solids*. John Wiley and Sons, New York, 1983, p. 135.
25. Berghmans, M., Thijs, S., Cornette, M., Berghmans, H., De Schryver, F. C., Moldenaers, P. and Mewis, J., *Macromolecules*, 1994, **27**, 7669.
26. Klein, M., Brulet, A. and Guenet, J. M., *Macromolecules*, 1990, **23**, 540.
27. Tanaka, T., Swislow, G. and Ohmine, I., *Phys. Rev. Lett.*, 1979, **42**, 103.
28. Bansil, R., Lal, J. and Carvalho, B. L., *Polymer*, 1992, **33**, 2961.
29. Ohkura, M., Kanaya, T. and Kaji, K., *Polymer*, 1992, **33**, 3686.
30. Stockmayer, W. H., *J. Chem. Phys.*, 1943, **11**, 45.
31. Flory, P. J., *Principles of Polymer Chemistry*. Cornell University Press, Ithaca, New York, 1953.
32. Pekcan, O., Yilmaz, Y. and Okay, O., *Polymer*, 1996, **37**, 2049.
33. Reinecke, H., Saini, A., Mijangos, C. and Guenet, J. M., *Macromolecules*, 1996, **29**, 4799.
34. Spevacek, J., Saini, A. and Guenet, J. M., *Macromol. Rapid Comm.*, 1996, **17**, 389.
35. Mal, S. and Nandi, A. K., *Langmuir*, 1998, **14**, 2238.
36. Belke, R. E. and Cabasso, I., *Polymer*, 1988, **29**, 1831.
37. Roerdink, E. and Challa, G., *Polymer*, 1980, **21**, 509.
38. Flory, P. J. and Weaver, E. S., *J. Am. Chem. Soc.*, 1960, **82**, 4518.
39. Lovinger, A. J., in *Developments in Crystalline Polymers—I*, ed. D. C. Basset. Applied Science Publishers, London, 1981, p. 195.
40. Hoffman, J. D. and Weeks, J. J., *J. Res. Natl. Bus. Stand., U.S.*, 1962, **66**, 13.
41. Nandi, A. K. and Mandelkern, L., unpublished work.
42. Datta, J. and Nandi, A. K., *Polymer*, 1998, **39**, 1921.
43. Hoffman, J. D., Miller, R. L., Marand, H. and Roitman, D. B., *Macromolecules*, 1992, **25**, 2221.
44. Welch, G. J., *Polymer*, 1974, **15**, 428.
45. Hanack, M., *Conformation Theory*. Academic Press, New York, 1965, p. 40.
46. Farmer, B. L., Hopfinger, A. J. and Lando, J. B., *J. Appl. Phys.*, 1972, **11**, 4293.